e-ISSN 2320 –7876 www.ijfans.org
Vol.11, Iss.9, Dec 2022

Research Paper

Structural, Optical and Magnetic properties of pure and Co doped $MnWO_4$ nano structures

Anitha.S and E.Thirumal

Department of Physics,Faculty of Arts and Science

Bharat institute of higher education and research, Chennai-73

Email: anithasthampi @email. Com esthirumal@email.com

Address for Correspondence

Anitha.S and E.Thirumal

Department of Physics,Faculty of Arts and Science

Bharat institute of higher education and research, Chennai-73

Email: anithasthampi @email. Com esthirumal@email.com

Abstract:

The structural, optical, and magnetic properties of pristine and Co doped Manganese Tungstate ($MnWO_4$) nanostructures prepared by precipitation process are investigated and reported here. The tetragonal structure of pure and Co doped $MnWO_4$ compounds is shown by X-Ray Diffraction (XRD) studies. The Scherrer equation was used to compute the crystallite size of the particles. Fourier Transform Infrared (FTIR) spectroscopy was used to analyse the appearance of metal oxide vibrations (Pb, W, O, and Co). The creation of agglomerated nano flakes of pure and Co doped $MnWO_4$ samples are confirmed by electron microscope pictures. optical spectra delivered the excellent optical absorption behaviour and calculated bandgap suggested that the interaction of dopants with host lattice. Magnetization investigations show that the paramagnetic character of the pure and Co doped compound and carrier generated exchange interactions. According to the findings, the tunability of magnetism in the $MnWO_4$ system at room temperature in relation to dopant concentration leads to the material being used to fabricate magneto-optical and electrical devices.

Key words: $MnWO_4$, chemical precipitation, Nano flakes, optical bandgap, Magnetism

e-ISSN 2320 –7876 www.ijfans.org
Vol.11, Iss.9, Dec 2022

Research Paper

1. Introduction

Multiferroic magnetoelectric compounds have attracted more research attention in recent years due to their novel physical properties resulting from the coexistence and mutual interaction of ferromagnetic and ferroelectric orders, as well as their potential for use as magnetoelectric sensors or memory chips [1]. MnWO4 has attracted special attention among metal tungstates because of its possible uses in a variety of sectors, including photo catalysts, optical fibres, photoluminescence, humidity sensors, and it has also been reported as a multiferroic material. [2-3]. It has a monoclinic crystal structure with a P2/c space group. MnWO4 is made up of endless zigzag chains that run parallel to the c-axis and contain edge-sharing MnO6 or WO6 octahedra. Mn2+ and W6+ ions are found in MnO6 and WO6 octahedra respectively. The 3D structure of MnWO4 is formed by sharing the octahedral corners of MnO4 and WO4 chains [4]. By neutron diffraction under zero magnetic field, MnWO4 undergoes three successive anti ferromagnetic (AF) phase transitions (AF1, AF2, and AF3). Partially chemical substitutions of magnetic (Co, Ni) and nonmagnetic (Zn) ions for Mn2+ have been realised, because the spin-spiral order is important in regulating both ferroelectric activity and magnetoelectric effects [5]. Many studies have been published on the synthesis of MnWO4 nanoparticles with various morphologies. Nano plates are made using a hydrothermal technique, and it has been shown that they can be used as humidity sensors [6]. Solvothermal synthesis was used to create spherical-like particles. [7,8], nanorods [9], nanofibers [10], nano cocoons [11], flowerlike micro-structures [12], and Urchinlike microspheres gathered by nanorods [13]. Flower-like particles by spray pyrolysis method [14]. To make manganese tungstate, a variety of synthesis processes have been used, the most straightforward and cost-effective of which is chemical precipitation.

As a result, the current work focuses on the chemical precipitation production of pure and Co doped $MnWO_4$ samples, as well as the characterisation of structural, optical, and magnetic behaviour. The presence of room temperature antiferromagnetism in the Co doped $MnWO_4$ system is noteworthy. The unique properties of the Co doped MnWO4 sample point to possible uses in magneto-optics.

e-ISSN 2320 –7876 www.ijfans.org
Vol.11, Iss.9, Dec 2022

Research Paper

2. Experimental

2.1 Starting materials

Analytical grade of (>99.0 % pure) Manganese acetate, Sodium tungstate tri hydrate, Cobalt (II) acetate tetra hydrate was supplied by M/s. Alfa Acer (Germany) and Fluka Chemie AG, Buchs, Switzerland.

2.2 Synthesis of $MnWO_4$ by precipitation process

Chemical precipitation was used to make nanocrystalline $MnWO_4$ powders. In appropriate amounts of DI water, stoichiometric amounts of Mn acetate and sodium tungstate were dissolved separately. Dropwise, using a burette, sodium tungstate solution was added to Mn acetate solution. The solution was agitated continuously for 5 hours, after which the precipitate was aged for 24 hours before being washed with DI, Ethanol, and Acetone using centrifugation. Following that, the precipitate was dispersed in acetone and ultrasonicated for 15 minutes. The product was then allowed to dry for 24 hours at room temperature. The powders were then crushed and stored at 120°C for 12 hours. Finally, the final product was calcined for 4 hours at 500 degrees Celsius to obtain nanocrystalline $MnWO_4$ molecules. This de-agglomeration phase was repeated once more, and the powder was then dried for roughly an hour under an infrared (IR) lamp [3].

Using a similar chemical precipitation approach, Co doped with $MnWO_4$ was synthesized. This process was quite similar as such of preparation of $MnWO_4$. However, Mn acetate solution was mixed with a stoichiometric ration of Co nitrate solution. The dopant concentration (Co) was chosen to correspond to that of the dopants (Co-5%, Co-10%, Co-15% and Co-20%)

2.3 Characterizations

Phase identification done by powder x-ray diffraction through PAN Analytical (Model: X'Pert PRO) diffractometer generating Cu-Kα radiation of wavelength 1.5406 A˚. Fourier Transform Infra-Red (FTIR) spectra are recorded using Shimadzu spectrograph (Model: 8700) over a range between 4,000 and 400 cm^{-1} at a scan rate of 20 cm^{-1} per second. Raman spectra are recorded in the range 50–1,000 cm^{-1} using a confocal micro-Raman microscope (Renishaw in Via Reflex) with 0.6 mW power of Ar ion laser source and excitation wavelength of 488 nm. Surface morphology and elemental composition is analysed using High Resolution by Scanning Electron Microscope (HR-SEM) instrument of FEI Quanta FEG 200 and Energy Dispersive X-ray Analysis (EDAX) Thermos Nicolet respectively. UV-Visible spectra are

recorded by SHIMAZDU (UV2450) spectrophotometer. Room temperature M–H curve parameters measurements are carried out using Vibrating Sample Magnetometer (Lakeshore VSM 7410)

3. RESULTS AND DISCUSSION

3.1 PHASE ANALYSIS

Figure 1 shows the XRD patterns of pure $MnWO_4$ samples as well as Co- 5% 10%, 15%, and 20% doped $MnWO_4$ samples. The monoclinic structure of $MnWO_4$ molecule with space group p 2/c is indexed to all detected diffraction peaks and relative intensities (JCPDS card no: 80-0134) [3, 15]. As the dopant concentration increased, the peak broadened, indicating that the Co ion interacts with the host lattice. The computed average crystallite size of the produced compounds is around 26 nm, with a modest drop in crystallite size as the Co concentration increases. This could be related to ionic radius differences and microstructural variability. The average crystallite size is calculated by Scherrer formula as given in equation

$$D = \frac{K\lambda}{\beta \cos\theta}$$

Where K = shape factor, β = Full width half maximum, λ = wavelength of Cu radiation (1.5418 Å), θ = Bragg angle (degree) [4,16].

The enlarged XRD pattern (Fig.1b) reveal the effect of dopant on peak broadening, this peak broadening reduces the crystallite size (Co-5%=24, Co-10%= 22, Co-15%= 20 Co-20% =19). Hence, from the XRD studies formation of pure single [13,17]. $MnWO_4$ compound and the dopant interact with Mn-W-O lattice doesn't alter the crystallographic phase of the nanostructures

e-ISSN 2320 –7876 www.ijfans.org
Vol.11, Iss.9, Dec 2022

Research Paper

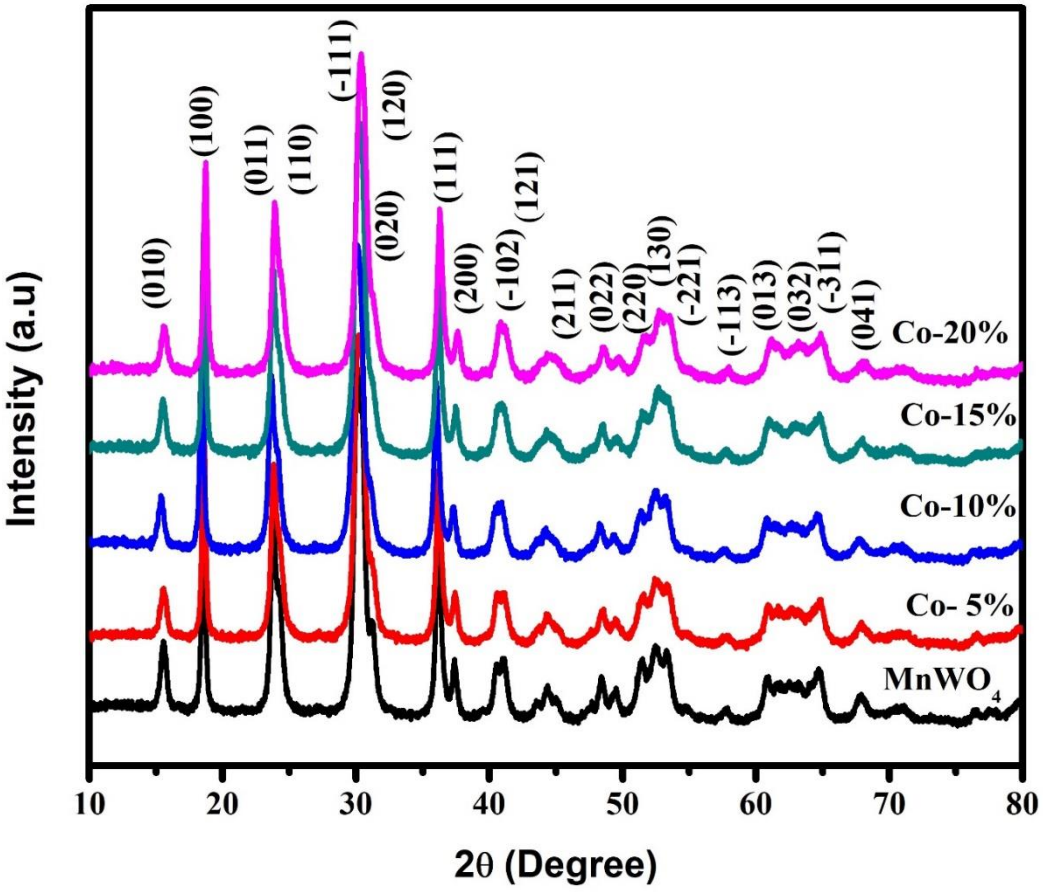

Figure 1a: XRD Pattern of pure and Co doped $MnWO_4$ nanostructures

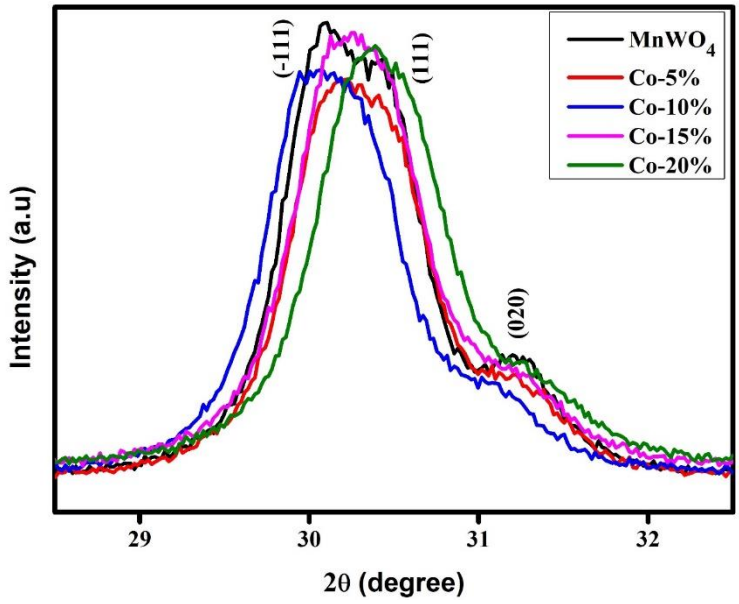

Figure 1b: Enlarged view of Plane (111) of pure and Co doped $MnWO_4$ nanostructures

e-ISSN 2320 –7876 www.ijfans.org
Research Paper
Vol.11, Iss.9, Dec 2022

3.2 FTIR Studies.

The illustration of FTIR spectra (Fig.2) of pure and Co doped $MnWO_4$ compounds. The broad band seen at 3430 cm-1 is suggestive of vibration of the O–H bond of the surface hydration, as shown in the picture. The deformation (H–O–H) vibration of the surface hydroxyl group is represented by the band at 1635 cm^{-1}. The symmetric and asymmetric stretching vibration modes of the W–O bond in the terminal WO_2 group of $MnWO_4$ correspond to the absorption peaks at 880 cm^{-1} and 819 cm^{-1}, respectively. The asymmetrical stretching vibrations of the W–O bond in the (W_2O_4) are shown by the strong band at 726 cm^{-1}, whereas the presence of stretching vibrations of the Mn–O bond is indicated by the strong band at 580 cm^{-1}. The band at 520 cm^{-1} was observed due to the presence of stretching vibration of Mn–O–Mn bond [18]

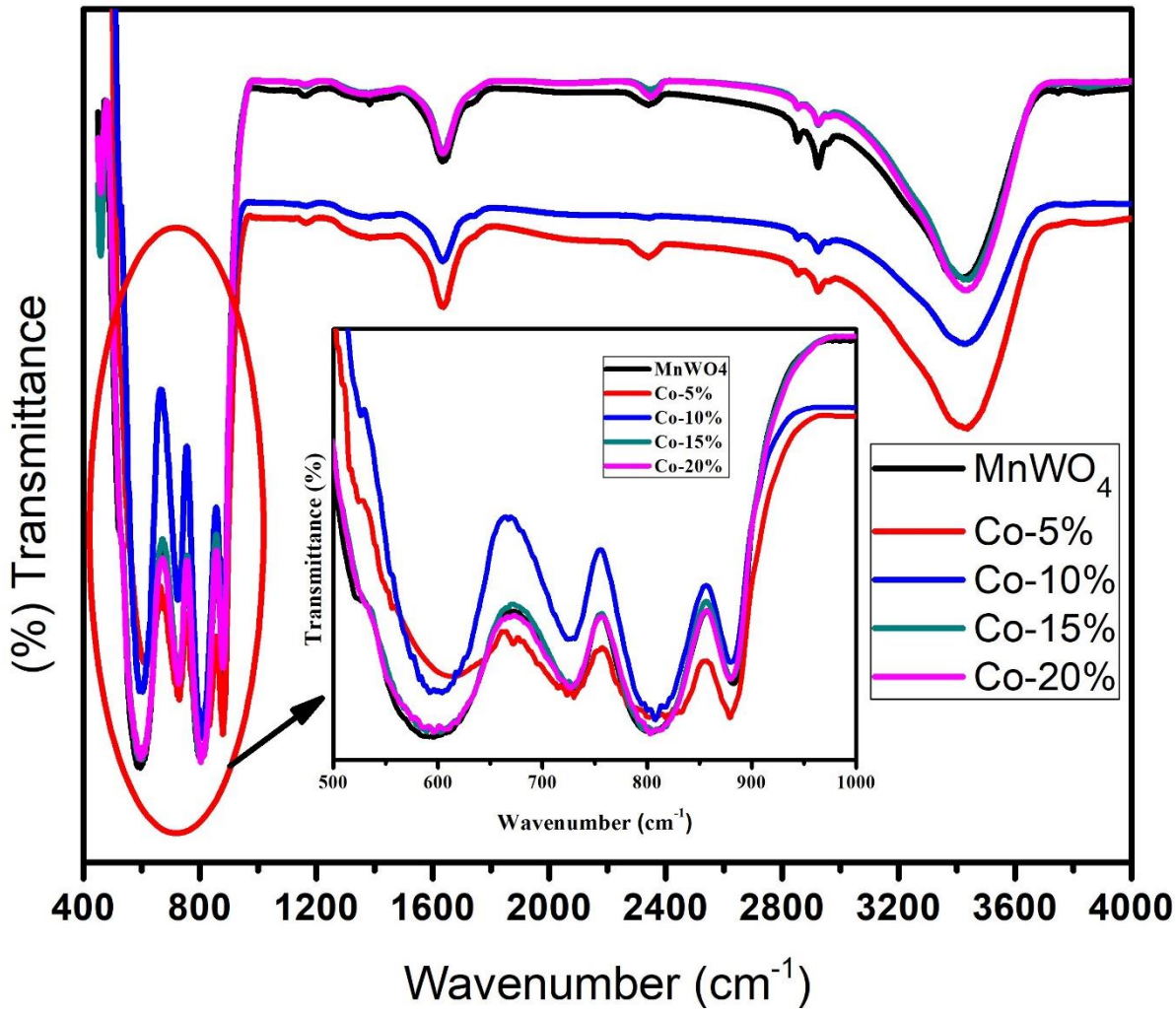

Figure 2: FTIR spectra of pure and Co doped $MnWO_4$ nanostructures

e-ISSN 2320 –7876 www.ijfans.org
Research Paper
Vol.11, Iss.9, Dec 2022

3.3 Raman analysis.

The Raman spectra of pure and Co doped $MnWO_4$ nanostructures are given (Fig. 3). The bands at 880, 698, 545, 380, 330, 258, 202 and 127 cm^{-1} were found for $MnWO_4$, which were acquired through distinct types of absorption at different translational levels [5,6]. The significant symmetric stretching of the WO^2 group in the $MnWO_4$ caused a very strong band to form at the 880 cm^{-1} area. The presence of mild asymmetric and symmetric stretching vibration modes of the W–O–W bond [5] is indicated by the bands at 698 cm^{-1}. Stretching vibration of Mn–O is responsible for the peak at 545 cm^{-1}. The presence of symmetric (W–O–W) stretching is indicated by the band at 380 cm^{-1}. W–O–W's scissoring is confirmed by the band at 330 cm^{-1}. The bending mode of $[WO_6]^{6-}$ is shown by a faint band at 202 cm^{-1}. The tungsten translational mode was represented by the bands at 127 cm^{-1} [19]. As a result, the fluctuation in Raman intensity implies that the local disorder has disrupted the lattice vibrations, confirming the proportionate incorporation of Co ions in the Mn-W-O lattice.

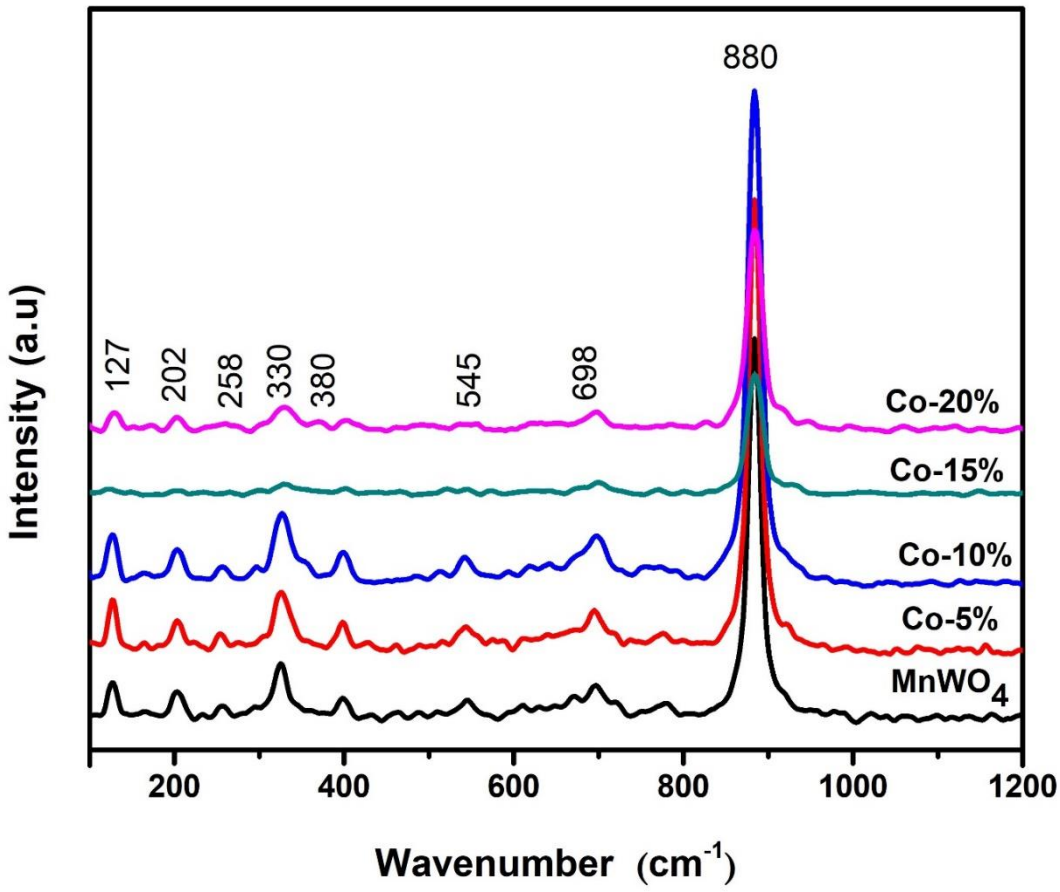

Figure 3: Raman spectra of pure and Co doped $MnWO_4$ nanostructures

e-ISSN 2320 –7876 www.ijfans.org
Research Paper
Vol.11, Iss.9, Dec 2022

3.4. Surface morphology and Elemental analysis.

Figure 4 shows HRSEM images of pure, Co-5% and Co-15%. The size of the particle is reduced, and the particles are agglomerated together, as shown in the micrographs. The size reduction is due to the first distortion created around the Co atom inside the Mn-W-O lattice [4, 20]. This could be due to the fact that particulate systems tend to agglomerate or develop into larger particles to reduce their surface free energy. EDS analysis is used to confirm the existence of dopants in a $MnWO_4$ lattice. Only the elements Mn, W, and O are present in the pure sample, according to the spectra. The presence of additional Co peaks and the absence of other contaminants are clearly seen in the doped sample.

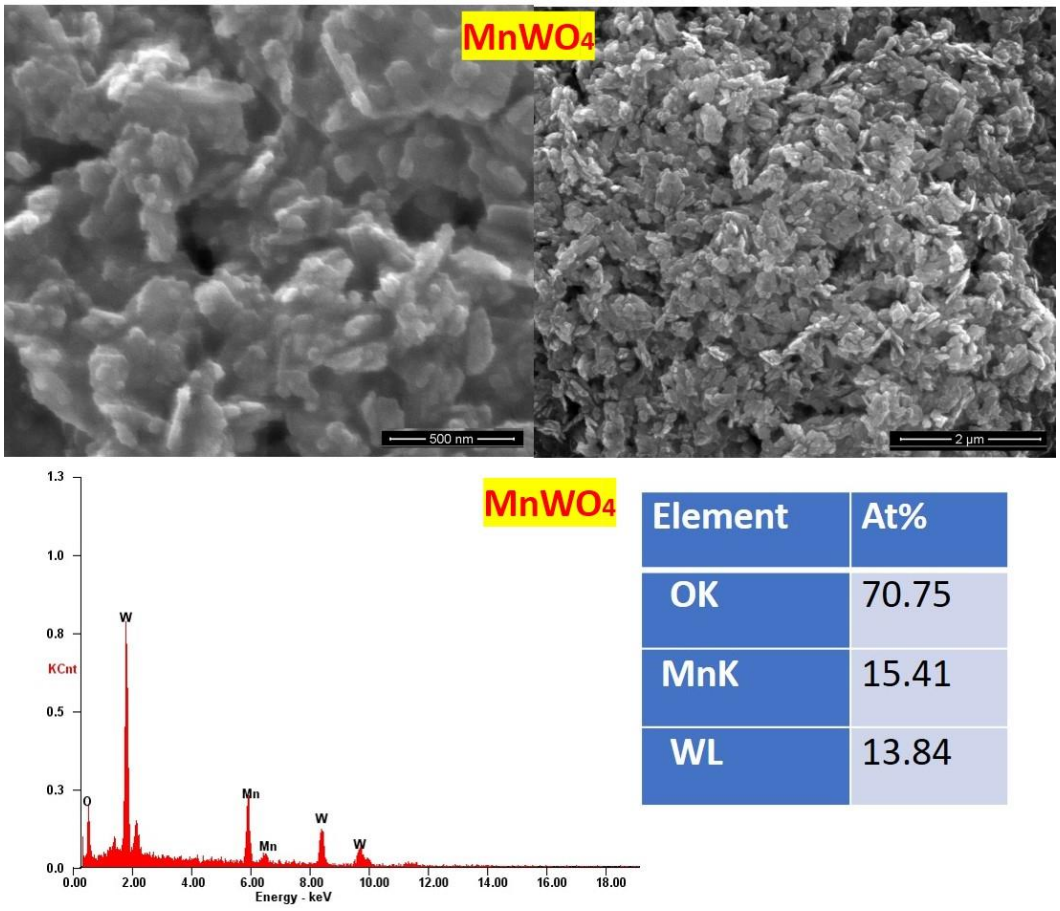

Element	At%
OK	70.75
MnK	15.41
WL	13.84

Figure 4a: SEM and EDS images of pure $MnWO_4$ nanostructures

e-ISSN 2320 –7876 www.ijfans.org
Research Paper
Vol.11, Iss.9, Dec 2022

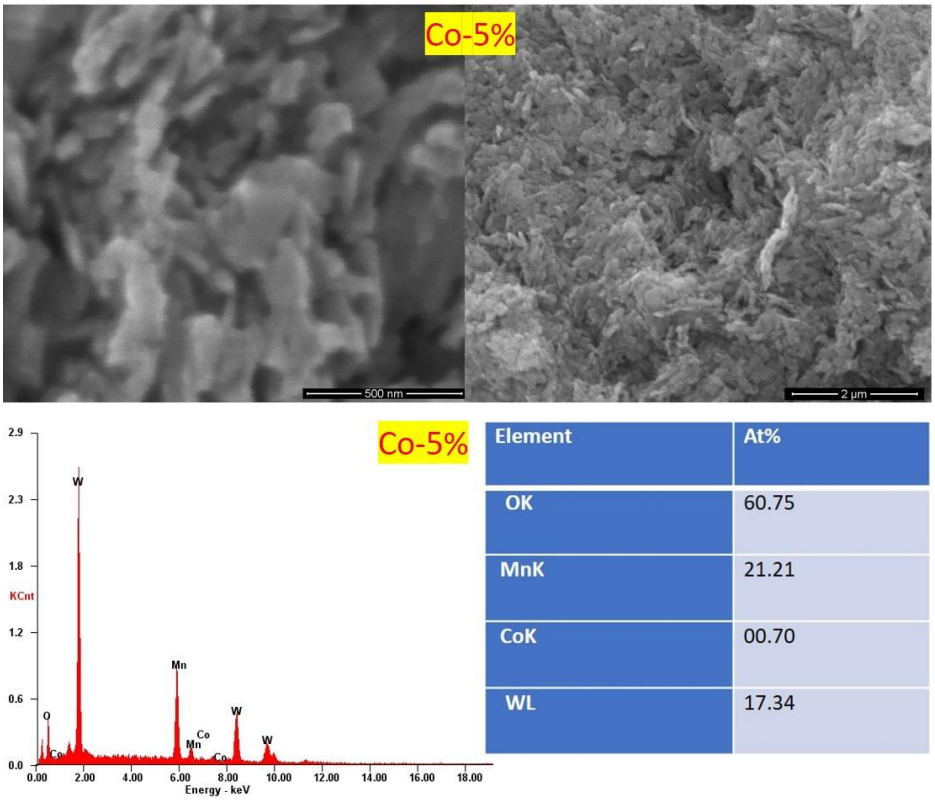

Element	At%
OK	60.75
MnK	21.21
CoK	00.70
WL	17.34

Figure 4b: SEM and EDS images of Co-5% doped $MnWO_4$ nanostructures

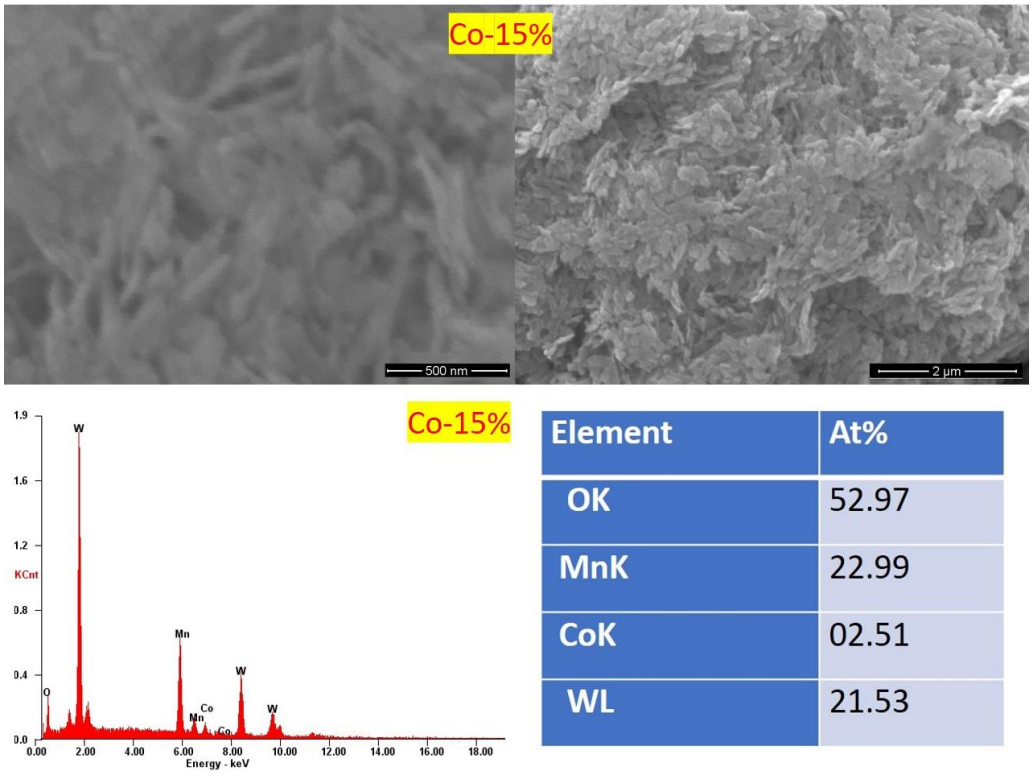

Element	At%
OK	52.97
MnK	22.99
CoK	02.51
WL	21.53

Figure 4c: SEM and EDS images of Co-15% doped $MnWO_4$ nanostructures

e-ISSN 2320 –7876 www.ijfans.org
Research Paper
Vol.11, Iss.9, Dec 2022

3.5. Optical studies.

Various factors, such as oxygen shortage, surface roughness, and impurity centers are likely to influence optical absorbance. Figure 5 shows the UV-visible optical absorption spectra of clean and Co doped materials. A high optical absorption peak was discovered about 260 nm, as seen in the image. The transition between the 2p oxygen state and the 3d Mn state determines the optical absorbance of $MnWO_4$. There is a minimal fluctuation in the absorbance intensity when Co ions are added to the host lattice, which increases as the function of dopant concentration increases. This means that Co doping in $MnWO_4$ causes significant lattice disruption. When Co- 5 percent is injected into the lattice, the absorption values climb to their maximum, as seen in the figure. This could be owing to the dopant-induced charge carriers. Furthermore, as the quantity of Co increases, the position of the optical absorption spectra shifts towards the lower wavelength. The Burstein–Moss effect [7,21] could explain the observed minor blue shift. With an increase in charge carriers, the Fermi level blends into the conduction band, and the optical band gap widens [8]. The optical energy band gap of $MnWO_4$ compounds were estimated by Tauc plot and found to be 2.51 eV, when the dopant concentration increases there was slight increase in the band gap (2.57 eV, 2.66 eV, 2.68 eV and 2.69 eV). This is may be due to quantum confinement effect, addition of dopant decreases the crystallite size and increases their bandgap.

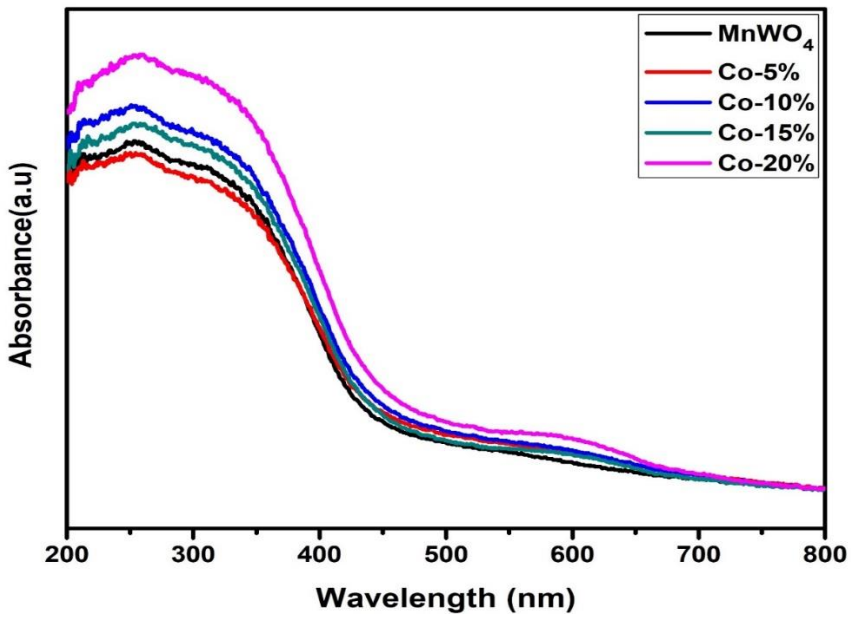

Figure 5: Optical absorption spectra pure and Co doped $MnWO_4$ nanostructures

e-ISSN 2320 –7876 www.ijfans.org
Research Paper
Vol.11, Iss.9, Dec 2022

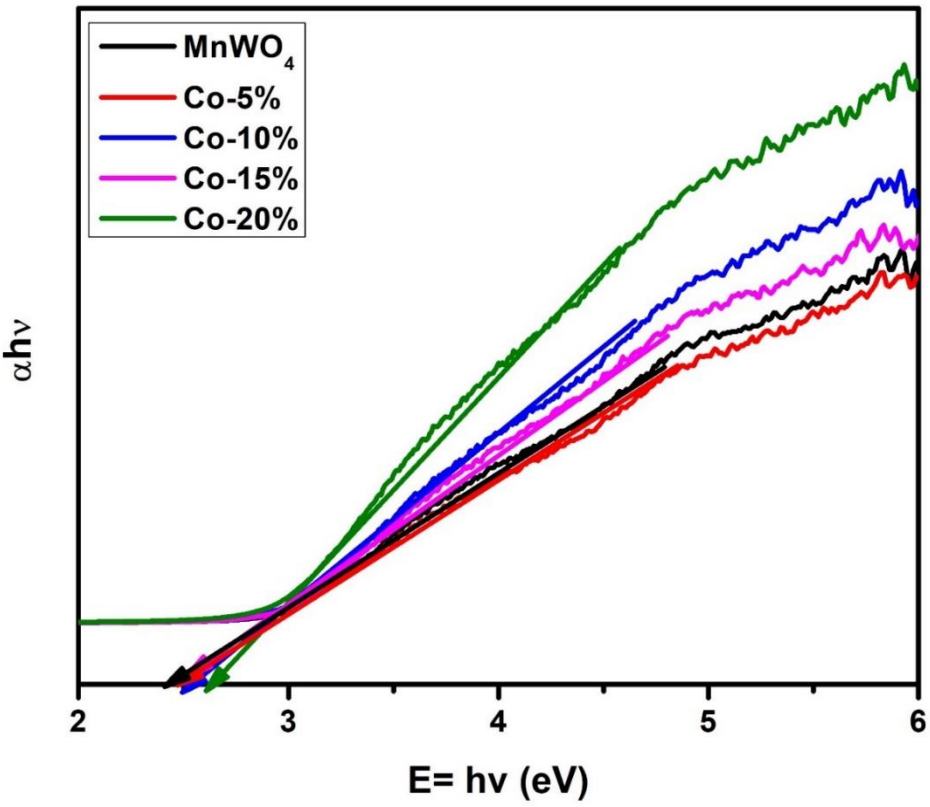

Figure 5b: Optical bandgap of pure and Co doped $MnWO_4$ nanostructures

3.6. Magnetic studies.

Room temperature M-H curve of pure and Co doped $MnWO_4$ compounds are shown in figure 3.6. From the magnetization studies, it is clearly observed the antiferromagnetic signature in all the prepared compounds. In general, metal tungstates exhibit the paramagnetic nature but in the present work all the synthesized compounds are in anti-ferromagnetic nature, it is already reported that the $MnWO_4$ compounds with magnetic cation Mn^{2+} belongs to antiferromagnetic materials [7 -9, 22]. In general, vacancy, defects and surface morphology of the compounds influences the magnetic properties. As the content of Co in the host lattice increases, there is a possible interaction between 3d spin states of Co, Mn 3d states and 4f state of W. Co interaction with Mn-W-O lattice provide a greater role in magnetic property [22]. Similarly, the incorporation of Co ions induces oxygen vacancies, which act as double electron donors, this may also influence the magnetic property of the prepared samples.

e-ISSN 2320 –7876 www.ijfans.org
Research Paper
Vol.11, Iss.9, Dec 2022

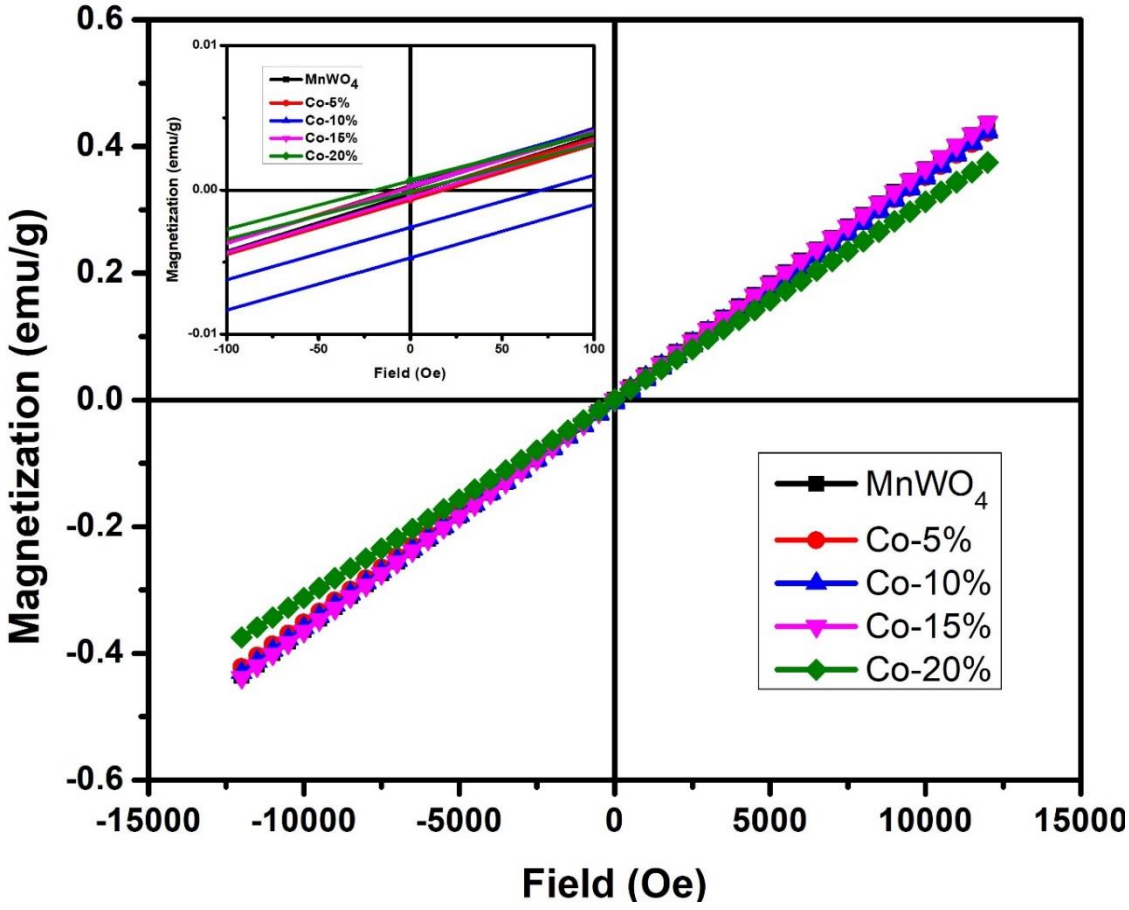

Figure 6: Magnetic studeis of pure and Co doped $MnWO_4$ nanostructures

4. Conclusion

A chemical precipitation method was used to synthesize the pure and Co doped $MnWO_4$ nano structures. XRD was used to establish the phase identification and monoclinic structure of the produced compounds. FTIR and Raman spectra investigations reveal the metal oxide vibrations (Mn-W-O) and local structural disorder characteristics. HRSEM revealed poly-dispersed and agglomeration particles for all the samples. The band gap corresponding to the significant optical absorption confirms the quantum confinement effect. Magnetic tests at room temperature revealed that all of the produced compounds have a paramagnetic signature and small hysteresis loop present in the low magnetic fields, which suggested that the co ions interact with host and produce some considerable defects in the samples. these defects are oriented along with the direction of magnetic field. The magnetic behaviour may understood in terms of defects and dopant ions present in the samples.

Reference

[1]. Vincent Hardy, Christophe Payen, Françoise Damay, Lynda Meddar, Michaël Josse and Gilles Andre, Phase transitions and magnetic structures in MnW_{1-x} $MoxO_4$ compounds ($x \leqslant 0.2$) J. Phys.: Condens. Matter 28 (2016), 336003.

[2]. V Felea, P Lemmens, S Yasin, S Zherlitsyn, K Y Choi, C T Lin and C Payen, J. Phys.: Condens. Matter 23 (2011), 216001.

[3]. Feihui Li, Xia yang, Xub, Jialei, Huo, Wei Wang, A simple synthesis of $MnWO_4$ nanoparticles as a novel energy storage material, Materials Chemistry and Physics, Vol. 167, (2015), pp.22-27.

[4]. O Heyer, N Hollmann, I Klassen, S Jodlauk, L Bohaty, P Becker, J A Mydosh, T Lorenz and D Khomskii, A new multiferroic material: $MnWO_4$, J. Phys.: Condens. Matter 18 (2006) L471–L475

[5]. S Muthamizh, R Suresh, K Giribabu, R Manigandan, S Praveen Kumar, S Munusamy, V Narayanan $MnWO_4$ nanocapsules: synthesis, characterization and its electrochemical sensing property, J. Alloys and Compounds 619 (2015) 601–609.

[6]. Lynda Meddar, Michael Josse, Philippe Deniard, Carole La, Gilles Andre, Francoise Damay, Vaclav Petricek, Stephane Jobic, Myung-Hwan Whangbo, Mario Maglione, and Christophe Payen, Chem. Mater. 21 (2009), 5203–5214.

[7] L. Zhang, C. Lu, Y. Wang, Y. Cheng, “Hydrothermal synthesis and characterization of $MnWO_4$ nanoplates and their ionic conductivity” Mater. Chem. Phys. 103 (2007) 433.

[8] W. Tong, L. Li, W. Hu, T. Yan, X. Guan, G. Li, J. “Systematic Control of Monoclinic $CdWO_4$ Nanophase for Optimum Photocatalytic Activity”, Phys. Chem. C 114 (2010) 15298.

[9] S.J. Chen, X.T. Chen, Z. Xue, J.H. Zhou, J. Li, J.M. Hong, X.Z. You, “Morphology control of MnWO4nanocrystals by a solvothermal route” J. Mater. Chem. 13 (2003) 1132.

[10] S. Lei, K. Tang, Z. Fang, Y. Huang, H. Zheng, “Synthesis of $MnWO_4$ nanofibers by a surfactant-assisted complexation–precipitation approach and control of morphology” Nanotechnology 16 (2005) 2407.

[11] W.B. Hu, X.L. Nie, Y.Zh. Mi, "Controlled synthesis and structure characterization of nanostructured $MnWO_4$", Mater. Charact. 61 (2010) 85.

[12] Y. Xing, S. Song, J. Feng, Y. Lei, M. Li, H. Zhang, "Microemulsion-mediated solvothermal synthesis and photoluminescent property of 3D flowerlike $MnWO_4$ micro/nanocomposite structure, Solid State Sci. 10 (2008) 1299.

[13] Y.X. Zhou, Q. Zhang, J.Y. Gong, S.H. Yu, "Surfactant-Assisted Hydrothermal Synthesis and Magnetic Properties of Urchin-like $MnWO_4$ Microspheres" J. Phys. Chem. C 112 (2008) 112.

[14] S. Thongtem, S. Wannapop, T. Thongtem, "Characterization of $MnWO_4$ with flower-like clusters produced using spray pyrolysis" Trans. Nonferrous Met. Soc. China 19, (2009) s100.

[15]. Lynda Meddar, Michael Josse, Mario Maglione, Amandine Guiet, Carole La, Philippe Deniard, Rodolphe Decourt, Changhoon Lee, Chuan Tian, Stephane Jobic, Myung-Hwan Whangbo and Christophe Payen, In. Chem. Mater. 24 (2012), 353−360.

[16]. Shingo Toyoda, Manfred Fiebig, Lea Forster, Taka-hisa Arima, Yoshinori Tokura & Naoki Ogawa, "Writing of strain-controlled multiferroic ribbons into $MnWO_4$, Nature Communications, Vol.12, pp 6199 (2021)

[17]. Ptak, M; Maczka, M; Hermanowicz, K; Pikul, A; Hanuza, J, Temperature-dependent Raman and IR studies of multiferroic $MnWO_4$ doped with Ni^{2+} ions" Spectrochimica Acta Part A 86 (2012) 85–92.

[18]. Wenming Tong, Liping Li, Wanbiao Hu, Tingjiang Yan, Xiangfeng Guan, and Guangshe Li, "Kinetic Control of $MnWO_4$ Nanoparticles for Tailored Structural Properties" J. Solid State Chem. 184 (2011) 2446–2457.

[19]. Mirosław Mączka, Maciej Ptak, Adam Pikul, Leszek Kępiński, Paweł E. Tomaszewski, Jerzy Hanuza "Phonon and magnetic properties of nanocrystalline $MnWO_4$ prepared by hydrothermal method" Vibrational Spectroscopy 58 (2012) 163–168.

[20] Mehdi Rahimi Nasrabadi1, Mohammad Eghbali Arani, "The effect of sugars on the morphology of $MnWO_4$ nanoparticles, and evaluating the product as photocatalysts" J Mater Sci: Mater Electron 28, (2017), 15239–15245.

[21] Pascaline Patureau, Michael Josse, Remi Dessapt, Jean-Yves Mevellec, Florence Porcher, Mario Maglione, Philippe Deniard and Christophe Payen, “Effect of Nonmagnetic Substituents Mg and Zn on the Phase Competition in the Multiferroic Antiferromagnet $MnWO_4$” Inorg. Chem. 54 (2015), 10623−10631.